

A ROLE OF THE REACTION KERNEL IN PROPAGATION AND STABILIZATION OF EDGE DIFFUSION FLAMES OF C₁-C₃ HYDROCARBONS

Fumiaki Takahashi

National Center for Microgravity Research on Fluids and Combustion, Cleveland, OH 44135

Viswanath R. Katta

Innovative Scientific Solutions, Inc., Dayton, OH 45440

INTRODUCTION

Diffusion flame stabilization is of essential importance in both Earth-bound combustion systems and spacecraft fire safety. Local extinction, re-ignition, and propagation processes may occur as a result of interactions between the flame zone and vortices or fire-extinguishing agents. By using a computational fluid dynamics code [1] with a detailed chemistry model for methane combustion, the authors have revealed [2-5] the chemical kinetic structure of the stabilizing region of both jet and flat-plate diffusion flames, predicted the flame stability limit, and proposed diffusion flame attachment and detachment mechanisms in normal and microgravity. Because of the unique geometry of the edge of diffusion flames, radical back-diffusion against the oxygen-rich entrainment dramatically enhanced chain reactions, thus forming a peak reactivity spot, i.e., *reaction kernel*, responsible for flame holding. The new results have been obtained for the edge diffusion flame propagation and attached flame structure using various C₁-C₃ hydrocarbons.

EXPERIMENT

Global observations of flames were made in the NASA Glenn 2.2-Second Drop Tower using a circular fuel tube (2.87 mm i.d. × 330 mm length) in a vented combustion chamber (255 mm i.d., × 533 mm length). A fuel jet was ignited at ~10 mm above the jet exit using a heated Nichrome wire immediately after dropping the rig for microgravity tests.

COMPUTATION

The time-dependent two-dimensional numerical code, developed by Katta et al. [1], is described elsewhere [3]. The C₃-chemistry model [6, 7] (33 species and 112 steps) includes C₁- or C₂-chemistry portions previously used [2-5]. A radiation model [8] based on an optically thin-media assumption and Plank's mean absorption coefficients was used for CO₂, H₂O, CH₄, and CO. The computational domain of 60 × 50 mm in the axial (*z*) × radial (*r*) directions is represented by a mesh of up to 601 × 201 with clustered grid lines near the jet exit with a minimum spacing of 0.05 mm. The inner diameter and lip thickness of the fuel tube are *d* = 3 mm and 0.5 mm, respectively. The fuel tube exit plane is placed 10 mm downstream from the inflow boundary in the open computational domain. Table 1 shows the test conditions. The fuel jet velocity of each fuel is determined based on the stoichiometric fuel requirement per unit volume of oxygen as same as that of methane (Case 1) studied previously [5]. The ambient air velocity is negligibly small (*U*_a = 0.001 m/s).

Table 1 Test conditions

Case	Fuel	<i>U</i> _i (m/s)	Gravity
1	Methane	0.1200	0g
2	Ethane	0.0686	0g
3	Ethylene	0.0800	0g
4	Acetylene	0.0960	0g
5	Propane	0.0480	0g
6	Ethane	0.0686	1g

RESULTS AND DISCUSSION

Figure 1 shows examples of video images of methane, ethane and propane flames in still air in microgravity at elapse times after ignition of $t = 2$ s. Spherical blue flames of nearly equal size were formed with the flame base approx. 3–4 mm below the jet exit and approx. 3–4 mm away from the burner wall. The weak methane flame has a larger quenched space. Soot formed initially at ignition disappeared completely for methane, almost diminished for ethane, but remained for propane. Each flame expanded slowly for the entire drop period ($t = \sim 2$ s).

Figure 2 shows the calculated temperature fields in ethane flames in 0g and 1g. In each case, the cold fuel jet issued for 0.3 s prior to ignition. The fuel jet was ignited at a centerline location where the stoichiometric mixture was formed. The edge of the flame propagated through the fuel-air mixing layer. Figure 3 shows the flame displacement velocity vector (\mathbf{v}_f) and its angle (θ_f) with respect to the horizon determined from the temperature field images for various fuels in 0g. Table 2 summarizes the average displacement velocities ($|\bar{v}_f|$) and the stoichiometric laminar flame speed (S_L) data in the literature [9]. There is an excellent correlation between these quantities as $|\bar{v}_f| = 0.9475S_L$ with $R = 0.99797$. This result is important because the computations were conducted using the identical detailed chemistry model for various fuels without adjusting chemical kinetic parameters and the propagating edge diffusion flame possessed the reaction

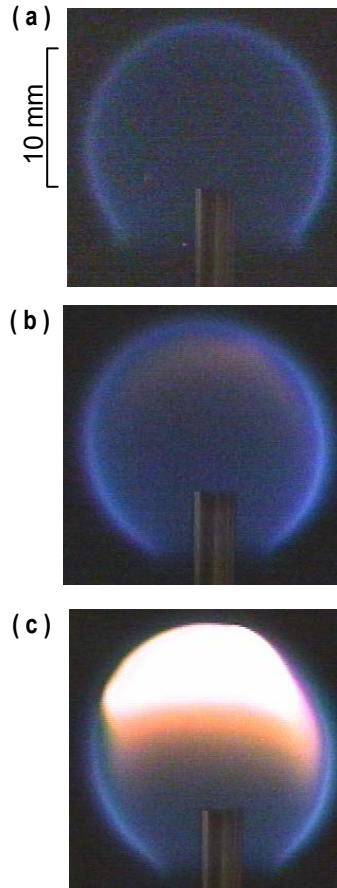
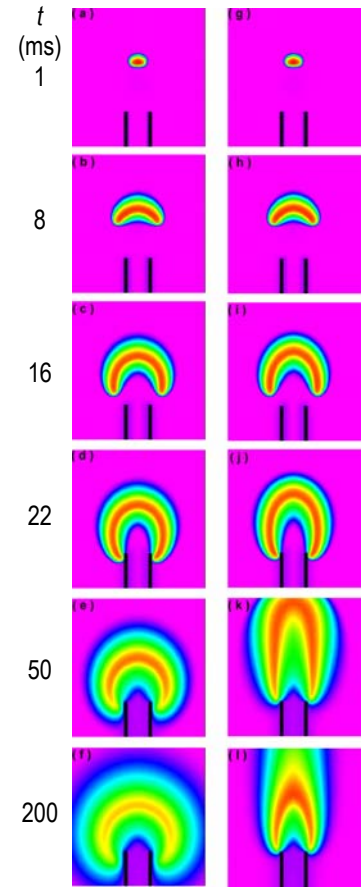


Fig. 1 Video images of (a) CH_4 , (b) C_2H_6 , and (c) C_3H_8 flames in μg . $t = 2$ s. .



0g (Case 2) 1g (Case 6)
Fig. 2 Calculated temperature field in ethane flames.

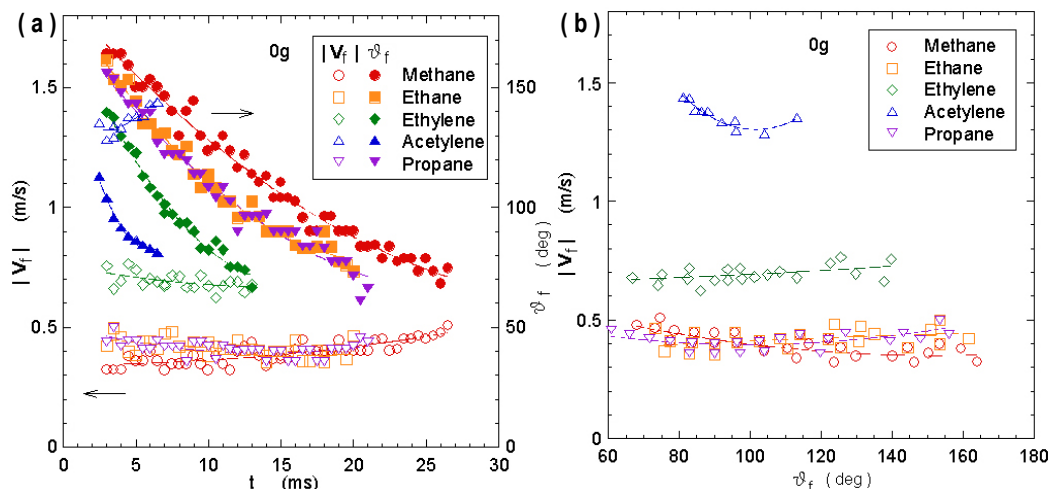


Fig. 3 Calculated flame displacement velocity and angle in the 0g flames (Cases 1-5).

kernel structure capable of consuming the reactants as fast as a stoichiometric premixed flame.

Figure 4 shows the structure of an ethane flame in 0g at the elapse time after ignition of 16 ms (see Fig. 1c), including the velocity vectors (\mathbf{v}), molar flux vectors of the H atom (\mathbf{M}_H), isotherms (T), total heat-release rate (\dot{q} , 20, 100, and 300 J/cm³s), and equivalence ratio (ϕ). The heat-release rate shows a peak reactivity spot (i.e., the reaction kernel) at the flame base. The \dot{q} , $|\mathbf{v}|$, and T at the reaction kernel were 378 J/cm³s, 0.0065 m/s, and 1436 K, respectively.

Figure 5 shows the variations of the species mole fractions (X_i), temperature, species formation rate ($\hat{\omega}_i$), and heat-release rate across the reaction kernel. The overall structure resembled to that of the 1g stationary methane flame with the standoff distance of several mm [4]. Besides the features of the radial diffusion-flame-like processes, the premixed combustion processes occurred at the center of the reaction kernel in the direction of the flame propagation. The reaction zone in the propagating flame broadened radially as a result of the thicker flammable mixture layer (~1.2 mm) formed in 0.3 s of the fuel-air mixing time, compared to the stationary flame (0.6-0.8 mm [4, 5]) with a short residence time (~0.01 s order) of the fluid particles over the standoff distance (4-9 mm) in a coflowing air (~0.7 m/s). For the C₂/C₃-fuels, the C₂-route in the oxidation process dominated over the C₁ route, and the C₂ exothermic reactions, $\text{CHCO} + \text{O} \rightarrow \text{CO} + \text{CO} + \text{H}$ (R59) and $\text{C}_2\text{H}_2 + \text{O} \rightarrow \text{CH}_2 + \text{CO}$ (R60) exceeded the C₁ reaction, $\text{CH}_3 + \text{O} \rightarrow \text{CH}_2\text{O} + \text{H}$ (R46), in contributing to the total heat-release rate.

Figures 6 and 7 show the structure of an attached ethane flame (Case 2) at $t=0.76$ s (\dot{q} : 30, 10, and 15 J/cm³s.). The flame shape, including the quenched space, matched the observation (Fig. 1b). The trend of the flame structure resembled to that of a methane flame [5], except that the C₂H₂ concentration in the high-temperature zone was an order of magnitude

Table 2 Flame displacement velocity

Fuel	$ \bar{v}_f $ (cm/s)	S_L (cm/s)
Methane	39.3 (0g)	43.4
Ethane	41.4 (0g)	44.5
	40.7 (1g)	
Ethylene	69.1 (0g)	68.0
Acetylene	136.2 (0g)	144
Propane	41.0 (0g)	45.6

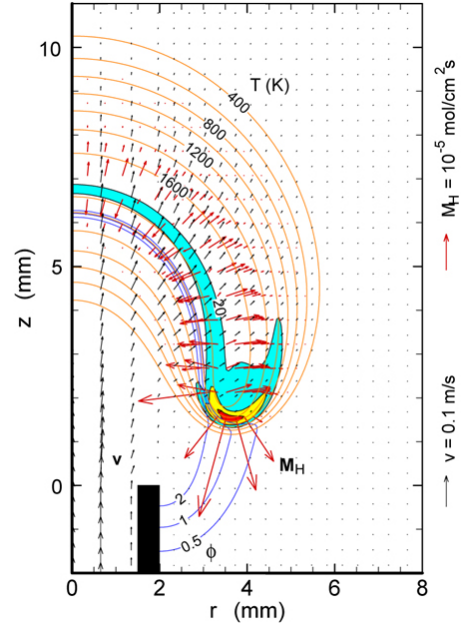


Fig. 4 Calculated propagating ethane flame structure in 0g (Case 2). $t = 16$ ms.

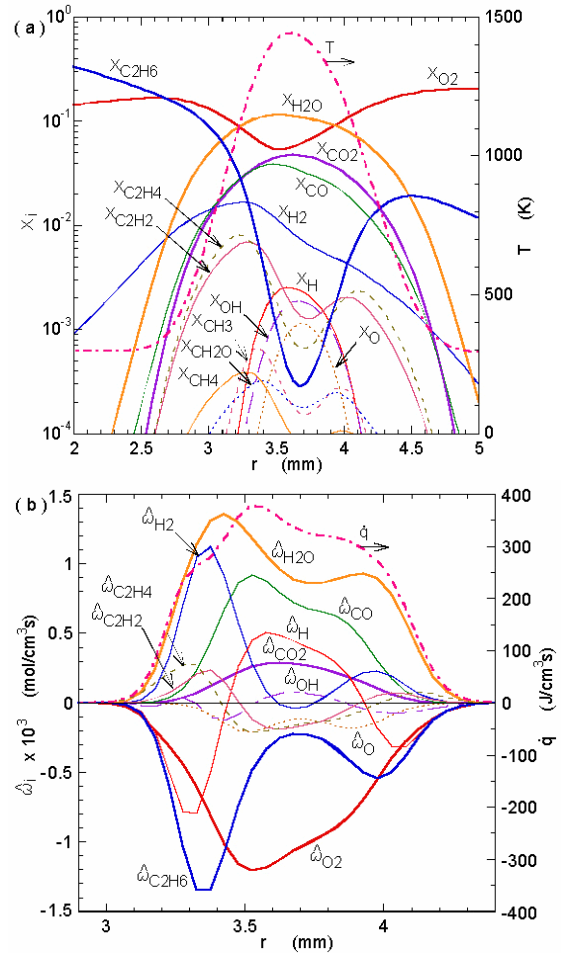


Fig. 5 Calculated flame structure across the reaction kernel (Case 2). $t = 16$ ms, $z = 1.58$ mm.

higher than that of the initial fuel. As a result, the fuel fragments burning near the peak temperature were C_2H_2 and H_2 , and CO was oxidized on the air side where radical-scavenging hydrocarbons disappeared.

CONCLUSIONS

Computations of C_1 - C_3 hydrocarbon jet flames using a detailed chemistry model have determined the edge diffusion flame displacement velocity after ignition in 1g and 0g environments. The calculated flame displacement velocity through the flammable mixture layer almost reached the stoichiometric laminar flame velocity for each fuel. The reaction kernel, which broadened radially facing the flammable mixture layer possesses a hybrid structure of diffusion and premixed flames in the lateral and longitudinal directions, respectively, with respect to the direction of the flame propagation. The structure of the reaction kernel in the attached flames of C_2 and C_3 hydrocarbons resembles to that of methane except for the high acetylene concentration in the peak-temperature region and the dominant C_2 -route oxidation pathway.

ACKNOWLEDGMENT

This work was supported in part by the NASA Office of Biological and Physical Research, Washington, DC, and in part by the U.S. Air Force Office of Scientific Research.

REFERENCES

1. Katta, V. R., Goss, L. P., and Roquemore, W. M., *AIAA J.* 32:84 (1994).
2. Takahashi, F. and Katta, V. R., *Proc. Combust. Inst.* 27:675 (1998).
3. Takahashi, F. and Katta, V. R., *Combust. Sci. Technol.* 155:243 (2000).
4. Takahashi, F. and Katta, V. R., *Proc. Combust. Inst.* 28:2071 (2000).
5. Takahashi, F. and Katta, V. R., *Proc. Combust. Inst.* 29: in press (2002).
6. Peters, N., in *Reduced Kinetic Mechanisms for Applications in Combustion Systems* (N. Peters and B. Rogg, Eds.), Springer-Verlag, Berlin, 1993, pp. 3-14.
7. Warnatz, J., in *Combustion Chemistry*, Springer-Verlag, New York, 1984, p. 197-360.
8. Annon., International Workshop on Measurement and Computation of Turbulent Nonpremixed Flames, <http://www.ca.sandia.gov/TNF/radiation.html>, 2001.
9. Glassman, I., *Combustion*, 3rd ed., Academic Press, San Diego, 1996.

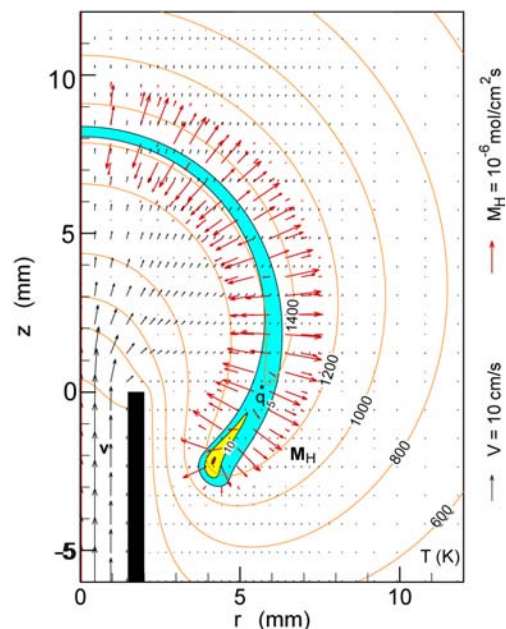


Fig. 6 Calculated attached ethane flame structure in 0g (Case 2). $t = 0.76$ s.

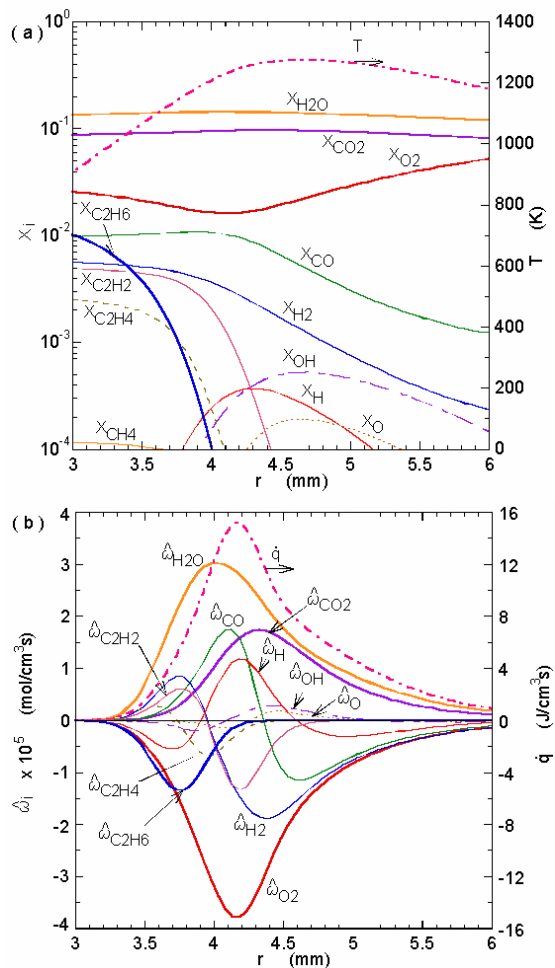


Fig. 7 Calculated flame structure across the reaction kernel (Case 2). $t = 0.76$ s, $z = -2.93$ mm.